

## Supplementary Information for

# Voltage-controlled skyrmion-based nanodevices for neuromorphic computing in a synthetic antiferromagnet

Ziyang Yu<sup>1</sup>, Maokang Shen<sup>2#</sup>, Zhongming Zeng<sup>3</sup>, Shiheng Liang<sup>4</sup>, Yong Liu<sup>1</sup>, Ming Chen<sup>1</sup>, Zhenhua Zhang<sup>1</sup>, Zhihong Lu<sup>5</sup>, Long You<sup>2</sup>, Xiaofei Yang<sup>2</sup>, Yue Zhang<sup>2\*</sup>, Rui Xiong<sup>1\*</sup>

1. Key Laboratory of Artificial Micro- and Nano-structures of Ministry of Education, School of Physics and Technology, Wuhan University, Wuhan, 430072, P. R. China
2. School of Optical and Electronic Information, Huazhong University of Science and Technology, Wuhan, 430074, P. R. China
3. Key Laboratory of Multifunctional Nanomaterials and Smart Systems, Suzhou Institute of Nano-Tech and Nano-Bionics, Chinese Academy of Sciences, Suzhou, Jiangsu, 215123, P. R. China
4. Department of Physics, Hubei University, Wuhan 430062, P. R. China.
5. The State Key Laboratory of Refractories and Metallurgy, School of Materials and Metallurgy, Wuhan University of Science and Technology, Wuhan, 430081, P. R. China

\*The corresponding author: Yue Zhang (E-mail: [yue-zhang@hust.edu.cn](mailto:yue-zhang@hust.edu.cn)) and Rui Xiong (E-mail: [xiongrui@whu.edu.cn](mailto:xiongrui@whu.edu.cn))

#The author who has the same contribution to Ziyang Yu

### S1. Influence of external electric field on the magnetic anisotropy constant

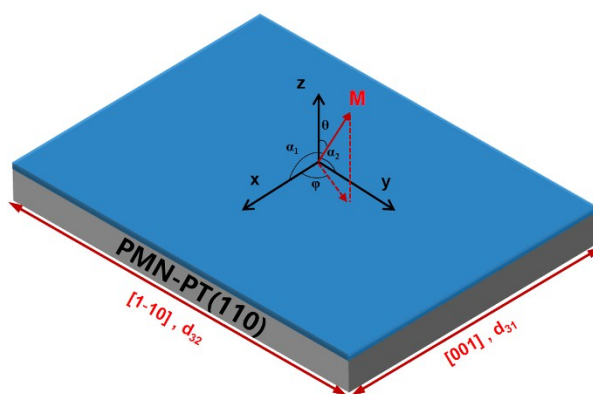


**Fig. S1. Spatial angles of the magnetic moment of the ultrathin ferromagnetic film with perpendicular magnetic anisotropy on the PMN-PT(110) substrate**

Variation of magnetic anisotropy energy under an external electric field for an ultrathin film with perpendicular magnetic anisotropy (PMA) is investigated quantitatively. Here, we consider an ultrathin film with PMA deposited on a PMN-PT(110) substrate (Fig. S1). The density of total magnetic anisotropy energy is:

$$F = K \sin^2 \theta - \frac{3}{2} \lambda_s (\sigma_1 \cos^2 \alpha_1 + \sigma_2 \cos^2 \alpha_2) - \frac{1}{2} \mu_0 M_s^2 \cos^2 \theta \quad (1).$$

Here  $K$ ,  $\theta$ ,  $\alpha_{1(2)}$ ,  $\sigma_{1(2)}$ ,  $\lambda_S$ ,  $\mu_0$ ,  $M_S$ , are uniaxial anisotropy constant, polar angle, the angle between magnetization and  $x(y)$  axis, the stress along  $x(y)$  axis, the saturation magnetostriction coefficient, vacuum permeability, and the saturation magnetization.

In a spherical coordinate system, Eq. (1) is converted into:

$$F = K_{\text{eff}} \sin^2 \theta$$

with 
$$K_{\text{eff}} = K - \frac{3}{2} \lambda_S \sigma_1 + \frac{3}{2} \lambda_S (\sigma_1 - \sigma_2) \sin^2 \varphi - \frac{1}{2} \mu_0 M_S^2 \quad (2).$$

Usually, the relationship between stress and electric field strength ( $E$ ) is nonlinear. However, when  $E$  is weaker than 0.5 kV/cm as indicated in the main text,  $\sigma(E)$  is very close to a linear function [S1]:

$$\begin{aligned} \sigma_1 &= \frac{Y}{1-\nu^2} (\nu d_{32} + d_{31}) E \\ \sigma_2 &= \frac{Y}{1-\nu^2} (\nu d_{31} + d_{32}) E \end{aligned} \quad (3).$$

Here  $Y$  and  $\nu$  are the Young's Modulus and Poisson's ratio, respectively, of the ultrathin magnetic film layer, and  $d_{31}$  and  $d_{32}$  are the piezoelectric constants of the single-crystal PMN-PT substrate in the  $x$  ([001]) and  $y$  ([1-10]) directions, respectively. Plugging Eq. (3) into (2), we finally derive the relationship between  $K_{\text{eff}}$  and  $E$  as:

$$K_{\text{eff}} = K - \frac{3}{2} \lambda_S \sigma_1 + \frac{3}{2} \lambda_S \frac{Y}{1+\nu} (d_{31} - d_{32}) E \sin^2 \varphi - \frac{1}{2} \mu_0 M_S^2 \quad (4).$$

Here  $Y$  and  $\nu$  are 180 GPa and 0.3, and  $\lambda_S$  and  $M_S$  for Pt/Co (CoFeB) PMA film are 290 ppm (110 ppm) and  $5.8 \times 10^5$  A/m ( $1.1 \times 10^6$  A/m) [S2-S5]. According to the experimental condition for electric field control of RKKY, the  $d_{31}$  and  $d_{32}$  for PMN-PT(110) are  $-1800$  pC/N and  $900$  pC/N, respectively [S6]. Based on these parameters, when  $E > 0$ , Eq. (4) is minimum for  $\varphi = \pi/2$ , and the  $K_{\text{eff}}$  is:

$$K_{\text{eff}} = K - \frac{3}{2} \lambda_S \sigma_2 - \frac{1}{2} \mu_0 M_S^2 \quad (5).$$

On the other hand, when  $E < 0$ , Eq. (4) is minimum for  $\varphi = 0$ , and the  $K_{\text{eff}}$  is:

$$K_{\text{eff}} = K - \frac{3}{2} \lambda_S \sigma_1 - \frac{1}{2} \mu_0 M_S^2 \quad (6).$$

In either case, when  $E$  is weaker than 0.5 kV/cm, the anisotropy constant contributed from stress is at the magnitude of  $10^2 \sim 10^3$  J/m<sup>3</sup>. The effective anisotropy constant for the demagnetization energy of Pt/Co (CoFeB) is  $2.1 \times 10^5$  J/m<sup>3</sup> ( $7.6 \times 10^5$  J/m<sup>3</sup>), and in general, the  $K$  for Pt/Co (CoFeB) is at the magnitude of  $10^6$  J/m<sup>3</sup> to ensure stable PMA. Therefore, the stress anisotropy energy contributes very little to the total magnetic anisotropy energy under such a weak electric field. Therefore, when  $E$  is weaker than 0.5 kV/cm as shown in the main text, it is reasonable that the variation of anisotropy constant can be neglected.

## S2. Energy stability of skyrmion in the multilayer

The total energy for the stable skyrmion system was derived from the simulation. Two sorts of skyrmions were considered. In one case the magnetic moments inside the skyrmion are parallel

to the magnetic moments in the lower layer (the ferromagnetic skyrmion (FM-Sky)), while it is on the contrary in the other case (the antiferromagnetic skyrmion (AFM-Sky)).

The results (Fig. S2) indicate that when the interlayer RKKY exchange coupling constant ( $J_{\text{ex}}$ ) is between  $-1 \times 10^{-7} \text{ J/m}^2$  and  $-3 \times 10^{-6} \text{ J/m}^2$ , the range of  $J_{\text{ex}}$  for the drastic changing of the radius of skyrmion, the energy for the stable FM-Sky is lower than that for the AFM-Sky. This proves that the FM-Sky-type skyrmion in the main text is stable in energy.

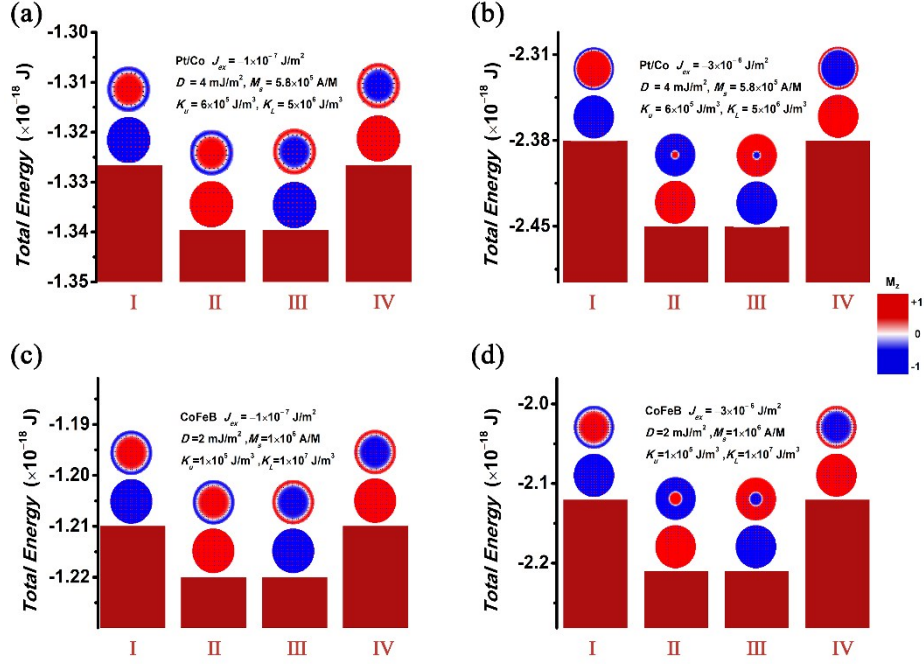


**Fig. S2. Comparison of total energy between an FM-Sky and an AFM-Sky: (a) Pt/Co with  $J_{\text{ex}} = -1 \times 10^{-7} \text{ J/m}^2$ ; (b) Pt/Co with  $J_{\text{ex}} = -3 \times 10^{-6} \text{ J/m}^2$ ; (c) CoFeB with  $J_{\text{ex}} = -1 \times 10^{-7} \text{ J/m}^2$ ; (d) CoFeB with  $J_{\text{ex}} = -3 \times 10^{-6} \text{ J/m}^2$**

### References:

- S1 M. Liu, O. Obi, J. Lou, Y. Chen, Z. Cai, S. Stoute, M. Espanol, M. Lew, X. Situ, K. S. Ziemer, V. G. Harris, and N. X. Sun, *Adv. Funct. Mater.*, 2009, **19**, 1826-1831.
- S2 G. A. Lebedev, B. Viala, T. Lafont, D. I. Zakharov, O. Cugat and J. Delamare, *Applied Physics Letters*, 2011, 99.
- S3 J. Sampaio, V. Cros, S. Rohart, A. Thiaville and A. Fert, *Nat. Nanotechnol.*, 2013, **8**, 839-844.
- S4 S. Iihama, Q. Ma, T. Kubota, S. Mizukami, Y. Ando and T. Miyazaki, *Appl. Phys. Express* 2012, **5**, 083001.
- S5 S. Luo, N. Xu, Z. Guo, Y. Zhang, J. Hong and L. You, *IEEE Electr Device L.* 2019, **40**, 635-638.
- S6 X. Wang, Q. Yang, L. Wang, Z. Zhou, T. Min, M. Liu and N. X. Sun, *Adv. Mater.*, 2018, 1803612.